

D. B. Pearson, Phys. Rev. Lett. **41**, 1361 (1978).

¹⁴See, for a summary, A. P. Kazantsev, Usp. Fiz. Nauk **124**, 113 (1978) [Sov. Phys. Usp. **21**, 58 (1978)].

¹⁵See, for a summary, S. Stenholm, Phys. Rep. C **43**, 151 (1978).

¹⁶R. J. Cook and A. F. Bernhardt, Phys. Rev. A **18**, 2533 (1978).

¹⁷R. J. Cook, Phys. Rev. Lett. **41**, 1788 (1978).

¹⁸B. P. Kibble, G. Copley, and L. Krause, Phys. Rev. **153**, 9 (1967).

¹⁹E. Arimondo, M. Inguscio, and P. Violino, Rev. Mod. Phys. **49**, 31 (1977).

²⁰G. A. Delone, V. A. Grinchuk, A. P. Kazantsev, and G. I. Surdutovich, Opt. Commun. **25**, 399 (1978).

Effects of Shape Resonances on Vibrational Intensity Distributions in Molecular Photoionization

Roger Stockbauer, B. E. Cole, and D. L. Ederer

National Measurement Laboratory, National Bureau of Standards, Washington, D. C. 20234

and

John B. West^(a)

Institute of Physical Science and Technology, University of Maryland, College Park, Maryland 20742

and

Albert C. Parr

Department of Physics and Astronomy, The University of Alabama, University, Alabama 35486

and

J. L. Dehmer

Argonne National Laboratory, Argonne, Illinois 60439

(Received 18 June 1979)

We report striking non-Franck-Condon vibrational intensity distributions associated with the shape resonance in the 5σ photoionization channel of CO. This example confirms the recent theoretical prediction that shape resonances will couple significantly with vibrational motion, leading to different resonance energies and profiles, and non-Franck-Condon intensities in alternative vibrational channels. Analogous effects are expected in connection with the widespread occurrence of shape resonances in both inner-shell and outershell molecular photoionization spectra.

The prominent role of shape resonances in molecular photoionization has gained wide recognition in the last few years. Their identification¹ in the innershell and outershell spectra of a growing, diverse collection of molecules has led to the study of their role in partial photoionization cross sections^{1d, 1e, 2} and photoelectron angular distributions.^{1d, 3} Recently, a new manifestation of shape resonances has been predicted⁴ by theoretical studies of the effects of vibrational motion on the quasibound states. In particular, shape resonances were found to induce significant coupling between the escaping photoelectron and the vibrational motion of the nuclei which is manifested as large, energy-dependent deviations from Franck-Condon (FC) vibrational intensity distributions over a broad spectral range encompassing the resonance. In this Letter, we present the first experimental evidence for this behavior in connection with the σ -type shape resonance in the

5σ photoionization channel of CO. This class of phenomena will play a central role in vibrationally resolved photoelectron studies conducted over the broad and continuous wavelength range afforded by synchrotron radiation sources.

The effect arises⁴ from the quasibound nature of the shape resonance, which is localized in a spatial region of molecular dimensions by a centrifugal barrier. This barrier and, hence, the energy and lifetime (width) of the resonance are sensitive functions of internuclear separation and vary significantly over a range of R corresponding to the ground-state vibrational motion. In an adiabatic treatment, the net dipole amplitude for a particular vibrational channel is obtained by averaging the R -dependent dipole amplitude, weighted by the product of the initial- and final-state vibrational wave functions at each R . Accordingly, transitions to alternative vibrational levels of the ion preferentially weight different

regions of R , leading to resonance positions and widths which vary with vibrational channel. When cast as ratios of vibrational intensities, this leads to large systematic deviations from the constant FC ratio which would result if the electronic and nuclear motion were uncoupled. This behavior was illustrated in Ref. 4 by a calculation for the $3\sigma_g$ photoionization channel of N_2 which exhibits the well-known^{1b, 1d-1f, 2b-2e} σ_u resonance at ~ 14 eV kinetic energy. In that calculation, the ($v=1$)/($v=0$) final-state vibrational intensity ratio is near the Franck-Condon factor (FCF) (9.3%)⁵ at threshold, falls slowly toward a minimum of 4% at ~ 9 eV kinetic energy, rises to a maximum of 30% at ~ 16 eV, and returns to a value near the FCF by 30 eV. At their respective peaks, the $v=1$ and 2 channels were found to be enhanced by factors of 3 and 10, respectively, suggesting that weaker levels experience larger shape-resonant enhancement. Equivalent effects are documented here for the analogous 5σ channel of the isoelectronic molecule CO, which we have chosen to study first since its resonance falls in a more convenient wavelength range, allowing us to map out the entire pattern of behavior outlined above.

The instrument used in this work is described in detail elsewhere⁶ and is only summarized briefly here: The new high-flux, 2-m, normal-incidence monochromator⁷ at the Synchrotron Ultraviolet Radiation Facility of the National Bureau of Standards was used for these measurements. This monochromator provides approximately 10^{10} photons $\text{sec}^{-1} \text{ \AA}^{-1}/\text{mA}$ of circulating current (typical initial current ~ 10 mA) at 1000 \AA and provides sufficient radiation for the present measurements down to ~ 375 \AA . The high flux is obtained by accepting ~ 65 mrad of the synchrotron radiation and by utilizing the small vertical dimension (~ 80 μm) of the stored electron beam as the entrance aperture of the monochromator. Together with a 1200-line/mm grating and a 200- μm exit slit, this configuration yields a photon resolution of ~ 0.8 \AA . The dispersed light is channeled by a 2-mm-i.d. capillary tube for a distance of 25 cm to the interaction region of the experimental chamber. The measured and calculated polarization of the light is $P \sim 0.60$ and is unaffected by the capillary light pipe. The electron energy analyzer is a rotatable, 2-in.-mean-radius, hemispherical device,⁸ operated at a constant resolution of ~ 100 meV full width at half maximum in these experiments. The light is horizontally polarized and, accordingly, the analyzer rotates in a plane perpendicular to the propagation

direction of the light, measuring a differential cross section given by

$$d\sigma/d\Omega = (\sigma/4\pi)[1 + \frac{1}{4}\beta(3P \cos 2\theta + 1)],$$

where P is the polarization of the light, σ is the integrated photoionization cross section, and β is the asymmetry parameter. This is a more convenient form of the equation given by Samson and Gardner^{9a} in which the trigonometric substitution $2 \cos^2\theta = \cos 2\theta + 1$ has been made. As we are concerned with relative intensity measurements in this work, we set the angle of observation at $\theta = 64^\circ$ to eliminate the term containing β in the above expression. Note that an inaccuracy in P of 20% would only alter this "magic" angle by 4° which is within the angular acceptance of the electron energy analyzer. The transmission of the analyzer was assumed to be equal for the alternative vibrational peaks.

The results are presented in Fig. 1 as ratios of intensities of the $v=1, 2,$ and 3 levels of $\text{CO}^+ X^2\Sigma^+$ to that of the ground vibrational state of the ion, as functions of incident photon energy. Immediately apparent in Fig. 1 is that, aside from the structures at ~ 19.5 eV to be discussed later, the gross pattern of spectral variation of these ratios strongly resembles that described above for the analogous states in N_2 . Specifically, the ($v=1$)/($v=0$) curve shows an oscillation with a minimum at ~ 21.4 eV and a maximum at ~ 22.3 eV and a peak-to-trough ratio of ~ 3 . The ($v=2, 3$)/($v=0$) curves are less well defined but clearly show successively greater enhancement at ~ 22 eV, relative to their weak background levels. Accordingly, we interpret the present results as the direct observation of the effects of shape resonances on vibrational intensity distributions. Previous measurements of ($v=1$)/($v=0$) obtained with a laboratory line source have been reported by Gardner and Samson^{9b}; however, the coarse mesh and scatter in their data do not permit identification of the systematic variation reported here. Note that the enhancement in the ratios centered at ~ 19.5 eV is far removed from the resonance position (~ 24 eV), does not fit into the simple pattern predicted by theory, and is very likely due to unresolved autoionization structure¹⁰ (converging to $\text{CO}^+ B^2\Sigma^+$ at 19.7 eV) in that portion of the spectrum. A large number of autoionization structures have also been observed¹¹ throughout the 22–26-eV region; however, these are extremely weak, doubly excited features, and are not expected to significantly affect the present results, which are dominated by one-

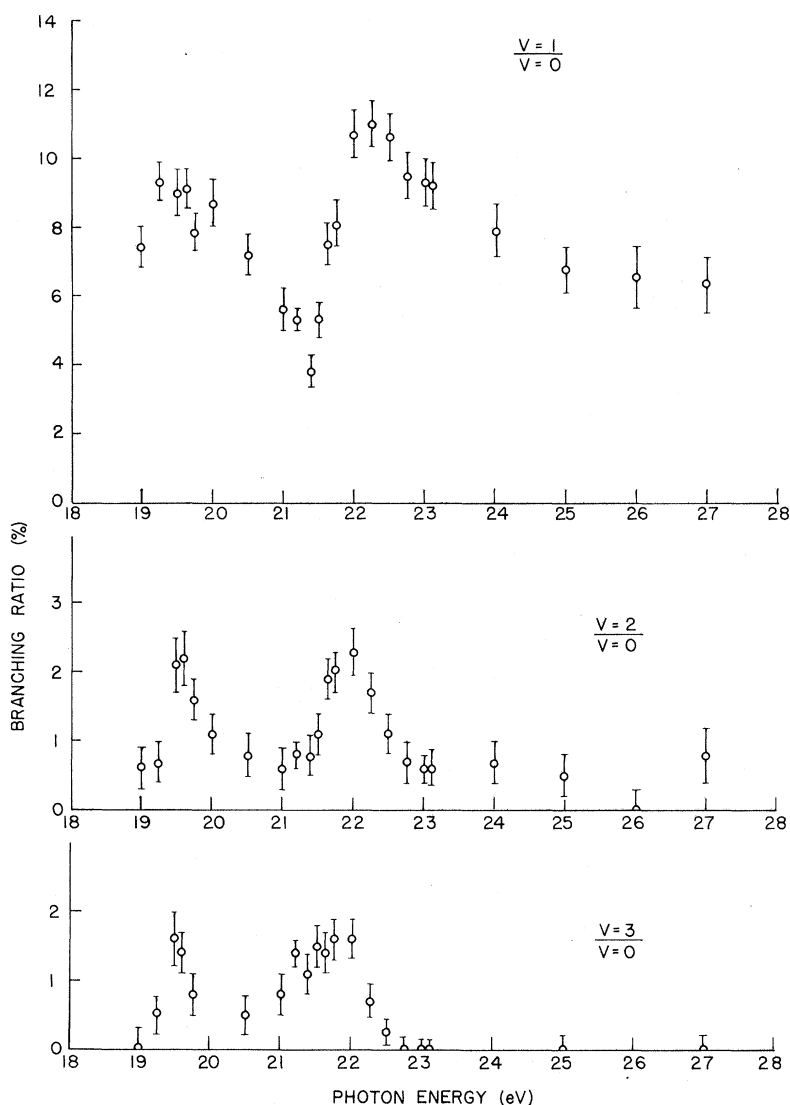


FIG. 1. Photoionization branching ratios for the $v = 0-3$ levels of $\text{CO}^+ X^2\Sigma^+$.

electron excitations.

Significant differences are also observed between the present results for CO and the theoretical results⁴ for N_2 . For example, the resonance maxima of the excited vibrational levels in Fig. 1 are near 22 eV or approximately 2 eV *below* the reported position of the shape resonance in the vibrationally unresolved 5σ band, which is dominated by the $v=0$ vibrational channel. In N_2 , the resonances in the vibrationally excited levels fall ~ 2 eV *above* the resonance in the unresolved band. We believe this reflects the differences in relative positions of the electronic potential energy curves for the two molecular systems. To see this, we note that in the R -dependent calculations⁴ for N_2 photoionization, the σ_u shape resonance

shifts to lower energy and becomes narrower when R is increased and shifts to higher energy and broadens when R is decreased. In N_2 , R_e for the $X^2\Sigma_g^+$ ionic state is slightly larger than that for the $X^1\Sigma_g^+$ neutral state, having the effect of preferentially weighting the low- R portion of the FC region. As a consequence the resonances in $v=1$ and 2 are shifted to higher energy than in $v=0$. In CO, the R_e of the $X^2\Sigma^+$ ionic state is slightly smaller than that of the $X^1\Sigma^+$ neutral state, so the observed opposite shift would appear consistent with the above argument. A calculation on CO would test this tentative interpretation. Another contrast is observed between the absolute values of the ratios in Fig. 1 and those reported⁴ for N_2 . For example, in the CO case the $(v=1)/$

($\nu = 0$) ratio is everywhere higher than the FCF (3.8%),⁵ except at the minimum at ~ 21.4 eV where the experimental curve dips near the FCF. In N_2 , on the other hand, the FC ratio appears to be the nonresonant background level about which the oscillation in ($\nu = 1$)/($\nu = 0$) varies. This may also reflect the subtle differences in the relative potential energy curves discussed above; however, we will not speculate further on this pending a direct comparison between experiment and theory in either CO or N_2 .

To summarize, we have shown (1) that a broad pattern of deviation from FC vibrational intensity distribution can be expected in the presence of a shape resonance; (2) that the pattern in CO qualitatively confirms a predicted pattern⁴ in N_2 ; and (3) that the observed behavior reflects the ν -dependent resonance profile and position which, in turn, depends on the relative positions and shapes of the initial- and final-state potential energy curves. These effects are a direct consequence of the enhanced coupling of electronic and nuclear motion caused by the temporary trapping of the photoelectron in the molecular core by a centrifugal barrier. Although different in detail, similar phenomena are expected to be associated with the widespread occurrence of shape resonances in innershell and outershell spectra of molecules, and are ideally suited for exploration by vibrationally resolved photoelectron spectroscopy using synchrotron radiation. We also wish to note the close relationship between the phenomenon described here and other shape-resonance-induced effects. The very same coupling between shape-resonant photoelectrons and nuclear motion is reflected in photoelectron angular distributions.⁴ Fragmentary experimental evidence¹² of this has recently been accounted for in prototype theoretical calculations⁴ and, as in the present case, sorely needs more systematic study. Another closely related phenomena is shape-resonance enhancement of vibrational excitation in electron-molecule scattering. Recent work¹³ has demonstrated the connection between intermediate-energy (10–40 eV) shape resonances in electron-molecule scattering and analogous resonances occurring 10–15 eV lower in kinetic energy in photoionization spectra. Hence, work on these three fronts can significantly extend and unify our understanding of the role of shape resonances in the continuum dynamics of molecules.

This work was supported in part by the U. S. Department of Energy. One of us (J.B.W.) is in receipt of a National Bureau of Standards Synchro-

tron Ultraviolet Radiation Facility Fellowship and one of us (A.C.P.) is a National Bureau of Standards Intergovernmental Personnel Act Appointee.

^(a)On detached duty from Daresbury Laboratory, Science Research Council, United Kingdom.

^{1a}See, e. g., J. L. Dehmer, *J. Chem. Phys.* **56**, 4496 (1972), and references therein.

^{1b}G. R. Wight, C. E. Brion, and M. J. van der Wiel, *J. Electron Spectrosc.* **1**, 457 (1973).

^{1c}G. R. Wight and C. E. Brion, *J. Electron Spectrosc.* **4**, 313 (1974).

^{1d}J. L. Dehmer and Dan Dill, *Phys. Rev. Lett.* **35**, 213 (1975), and *J. Chem. Phys.* **65**, 5327 (1976).

^{1e}J. W. Davenport, *Phys. Rev. Lett.* **36**, 945 (1976).

^{1f}A. Bianconi, H. Peterson, F. C. Brown, and R. Z. Bachrach, *Phys. Rev. A* **17**, 1907 (1978).

^{1g}A. P. Hitchcock and C. E. Brion, *J. Electron Spectrosc.* **15**, 201 (1979).

^{2a}See, e. g., J. A. R. Samson and J. L. Gardner, *J. Electron Spectrosc.* **8**, 35 (1976).

^{2b}J. A. R. Samson, G. N. Haddad, and J. L. Gardner, *J. Phys. B* **10**, 1749 (1977).

^{2c}E. W. Plummer, T. Gustafsson, W. Gudat, and D. E. Eastman, *Phys. Rev. A* **15**, 2339 (1977).

^{2d}T. N. Rescigno and P. W. Langhoff, *Chem. Phys. Lett.* **51**, 65 (1977).

^{2e}T. N. Rescigno, C. F. Bender, B. V. McKoy, and P. W. Langhoff, *J. Chem. Phys.* **68**, 970 (1978).

^{2f}N. Padial, G. Csanak, B. V. McKoy, and P. W. Langhoff, *J. Chem. Phys.* **69**, 2992 (1978).

^{2g}T. Gustafsson, *Phys. Rev. A* **18**, 1481 (1978).

^{2h}H. Levinson, T. Gustafsson, and P. Soven, *Phys. Rev. A* **19**, 1089 (1979).

³J. W. Davenport, Ph.D. thesis, University of Pennsylvania, 1976 (unpublished); D. Dill, S. Wallace, J. Siegel, and J. L. Dehmer, *Phys. Rev. Lett.* **41**, 1230 (1978), and **42**, 411(E) (1979); G. V. Marr, J. M. Morton, R. M. Holmes, and D. G. McCoy, *J. Phys. B* **12**, 43 (1979); S. Wallace, D. Dill, and J. L. Dehmer, to be published.

⁴J. L. Dehmer, D. Dill, and S. Wallace, to be published.

⁵D. L. Albritton, private communication.

⁶A. C. Parr, R. L. Stockbauer, B. E. Cole, D. L. Ederer, J. L. Dehmer, and J. B. West, to be published.

⁷D. L. Ederer, B. E. Cole, and J. B. West, to be published.

⁸J. L. Dehmer and Dan Dill, *Phys. Rev. A* **18**, 164 (1978).

^{9a}A. R. Samson and J. L. Gardner, *J. Opt. Soc. Am.* **62**, 856 (1972).

^{9b}J. L. Gardner and J. A. R. Samson, *J. Electron Spectrosc.* **13**, 7 (1978).

¹⁰G. R. Cook, P. H. Metzger, and M. Ogawa, *Can. J. Phys.* **43**, 1706 (1965).

¹¹K. Codling and A. W. Potts, *J. Phys. B* **7**, 163 (1974), and references therein.

¹²T. A. Carlson and A. E. Jonas, *J. Chem. Phys.* **55**, 4913 (1971); T. A. Carlson, *Chem. Phys. Lett.* **9**, 23

(1971); R. Morgenstern, A. Niehaus, and M. W. Ruf, in *Abstracts of Papers, Proceedings of the Seventh International Conference on the Physics of Electronic and Atomic Collisions, 1971*, edited by L. Branscom *et al.* (North-Holland, Amsterdam, (1971), p. 167.

¹³See, e. g., J. L. Dehmer, J. Siegel, and D. Dill, *J. Chem. Phys.* **69**, 5205 (1978); J. L. Dehmer, J. Siegel, J. Welch, and D. Dill, *Phys. Rev. A* (to be published); D. Dill, J. Welch, J. L. Dehmer, and J. Siegel, to be published.

Resonant Multiphoton Dissociation and Mechanism of Excitation for Ethyl Chloride

Hai-Lung Dai, A. H. Kung, and C. Bradley Moore

Department of Chemistry, University of California, and Materials and Molecular Research Division of the Lawrence Berkeley Laboratory, Berkeley, California 94720

(Received 6 February 1979)

Multiphoton dissociation of ethyl chloride was studied using a tunable 3.3- μm laser to excite CH stretches. Resonances in multiphoton dissociation yields match the position and shape of peaks in the fundamental, as narrow as 0.4 cm^{-1} , and first- and second-overtone absorption spectra. Transitions through the discrete levels occur at or near resonance. Anharmonicity is compensated by the presence of five CH stretch modes.

The many recent experimental and theoretical studies of collisionless multiphoton dissociation (MPD) by CO_2 lasers have established a good semiquantitative understanding of MPD for SF_6 and similar molecules.¹⁻⁵ The excitation of hydrogen stretching modes provides a qualitatively different situation. The anharmonicity is much larger; the quantum is a much larger fraction of the dissociation energy; the modes may be relatively weakly coupled to lower-frequency vibrations. Qualitatively new phenomena in MPD result.

Typical MPD spectra recorded with CO_2 lasers exhibit widths which are greater than entire fundamental vibration-rotation bands and red shifts which are comparable to *P*-branch half-widths. In the case of C_2H_4 multiphoton-absorption spectra have been recorded at high resolution. At the high intensities required for MPD, resonances were broadened to 10-20 cm^{-1} .⁶ A peak 10 cm^{-1} wide has been reported for cyclopropane at the 3102- cm^{-1} *Q* branch.⁷ Here we find for the first time sharp resonances in high-resolution yield spectra. Since these resonances match those found in ordinary absorption spectra, the optimum selectivity and laser frequency for isotope enrichment and chemical purification may be predicted from these spectra. The spectra give a detailed picture of the transition from discrete to quasicontinuous states.

In these experiments MPD of ethyl chloride, $\text{C}_2\text{H}_5\text{Cl} \rightarrow \text{C}_2\text{H}_4 + \text{HCl}$, is studied. Only seven photons $\nu \geq 2900 \text{ cm}^{-1}$ are needed to overcome the activation energy of $58 \pm 2 \text{ kcal/mole}$.⁸ A neodymium-doped yttrium aluminum garnet-laser-pumped LiNbO_3 optical parametric oscillator⁹

(OPO) provided the photolysis pulses. With an etalon in the OPO cavity the 3.3- μm pulse had a full width at half maximum of $0.15 \pm 0.03 \text{ cm}^{-1}$ and is 10 ns between half-power points. With a 0.75-m SPEX monochromator and a simple spectrophone cell containing 2 Torr of $\text{C}_2\text{H}_5\text{Cl}$ the laser frequency was determined relative to sharp features in the linear absorption spectrum to $\pm 0.1 \text{ cm}^{-1}$. The energy of the laser pulse, and occasionally the frequency, is monitored continuously during photolysis. The 3.3- μm beam is focused by a 5-cm-focal-length CaF_2 lens to a spot size of 0.6 mm full width at half maximum. The beam diameter is less than 0.9 mm over a distance of 7.5 mm. A 14-mm-thick glass cell with parallel NaCl windows attached by Torrseal epoxy is placed at Brewster's angle in the beam focus. For the data shown pulse energies ranged between $E_p = 2.7$ and 3.5 mJ. In this energy range the dissociation yield is proportional to $E_p^{3.5}$. At 3.5 mJ the peak intensity in the center of the focus is 120 MW/cm^2 . The effective photolysis volume at the focus is $1.6 \times 10^{-3} \text{ cm}^3$. Between 3000 and 7200 pulses were used for each photolysis. The photolysis products are analyzed with a flame-ionization gas chromatograph (Varian model No. 3700) with picogram sensitivity. Ethylene is the only hydrocarbon observed as a product; thus simple HCl elimination is the only reaction. Flame ionization is not sensitive to HCl. The relative dissociation yield $W_d(\nu)$ is given by the total area beneath the gas chromatograph peak, normalized by gas pressure (1.65 to 1.72 Torr), number of pulses, and $E_p^{3.5}$. An absolute calibration of the gas chromatograph combined with the effective-focal-volume estimate gives an *approximate*